

# Photodynamic therapy with conventional and PEGylated liposomal formulations of mTHPC (temoporfin): comparison of treatment efficacy and distribution characteristics in vivo

Vadzim Reshetov<sup>1-3</sup>  
 Henri-Pierre Lassalle<sup>1,2</sup>  
 Aurélie François<sup>1,2,4</sup>  
 Dominique Dumas<sup>5</sup>  
 Sebastien Hupont<sup>5</sup>  
 Susanna Gräfe<sup>6</sup>  
 Vasco Filipe<sup>7</sup>  
 Wim Jiskoot<sup>7</sup>  
 François Guillemin<sup>1,2,4</sup>  
 Vladimir Zorin<sup>3</sup>  
 Lina Bezdetsnaya<sup>1,2,4</sup>

<sup>1</sup>Université de Lorraine, Centre de Recherche en Automatique de Nancy, Campus Sciences, Vandœuvre-lès-Nancy, France; <sup>2</sup>Centre National de la Recherche Scientifique, Centre de Recherche en Automatique de Nancy, France; <sup>3</sup>Laboratory of Biophysics and Biotechnology, Physics Faculty, Belarusian State University, Minsk, Belarus; <sup>4</sup>Lorraine Cancer Institute, Vandœuvre-lès-Nancy, France; <sup>5</sup>Université de Lorraine, Plate forme d'Imagerie et de Biophysique Cellulaire Plate Forme IBI SA d'Imagerie et de Biophysique Cellulaire de Nancy, Centre National de la Recherche Scientifique, Vandœuvre-lès-Nancy, France; <sup>6</sup>Biolitec Research GmbH, Research and Development, Jena, Germany; <sup>7</sup>Division of Drug Delivery Technology, Leiden/Amsterdam Center for Drug Research, Leiden University, Leiden, the Netherlands

Correspondence: Vadzim Reshetov  
 Laboratory of Biophysics and Biotechnology, Physics Faculty, Belarusian State University,  
 4 Nezavisimosti Ave, 220030 Minsk, Belarus/RUE Belmedpreparaty,  
 30 Fabritsius St, 220007 Minsk, Belarus  
 Tel +375 29 346 88 56  
 Fax +375 17 220 31 42  
 Email vadim.reshetov@gmail.com

**Abstract:** A major challenge in the application of a nanoparticle-based drug delivery system for anticancer agents is the knowledge of the critical properties that influence their in vivo behavior and the therapeutic performance of the drug. The effect of a liposomal formulation, as an example of a widely-used delivery system, on all aspects of the drug delivery process, including the drug's behavior in blood and in the tumor, has to be considered when optimizing treatment with liposomal drugs, but that is rarely done. This article presents a comparison of conventional (Foslip<sup>®</sup>) and polyethylene glycosylated (Fospeg<sup>®</sup>) liposomal formulations of temoporfin (meta-tetra[hydroxyphenyl]chlorin) in tumor-grafted mice, with a set of comparison parameters not reported before in one model. Foslip<sup>®</sup> and Fospeg<sup>®</sup> pharmacokinetics, drug release, liposome stability, tumor uptake, and intratumoral distribution are evaluated, and their influence on the efficacy of the photodynamic treatment at different light–drug intervals is discussed. The use of whole-tumor multiphoton fluorescence macroscopy imaging is reported for visualization of the in vivo intratumoral distribution of the photosensitizer. The combination of enhanced permeability and retention-based tumor accumulation, stability in the circulation, and release properties leads to a higher efficacy of the treatment with Fospeg<sup>®</sup> compared to Foslip<sup>®</sup>. A significant advantage of Fospeg<sup>®</sup> lies in a major decrease in the light–drug interval, while preserving treatment efficacy.

**Keywords:** mTHPC, liposomes, drug release, liposomal pharmacokinetics, biodistribution, photodynamic therapy

## Introduction

Application of drug nanocarriers, including liposomes, has become one of the major directions of anticancer research.<sup>1-3</sup> The advantages of nanotherapeutics over conventionally formulated drugs include higher tumor accumulation due to the enhanced permeability and retention (EPR) effect, targeted delivery, higher efficacy, and reduced side effects. Liposomes were among the first nanoparticles proposed for drug formulation in medicine.<sup>3</sup> Significant advantages of liposomes have inspired the study of their application in photodynamic therapy (PDT) of cancer.<sup>4,5</sup> PDT is a minimally-invasive photochemical-based approach that uses a combination of a light-activated drug (photosensitizer) and the light of a specific wavelength to damage the target tumor tissue by generating reactive oxygen species.<sup>6</sup> The photosensitizer is generally administered intravenously, and the tumor is irradiated with a suitable light source after a certain time delay termed the drug–light interval (DLI).

Temoporfin, or meta-tetra(hydroxyphenyl)chlorin (mTHPC) is a highly efficient photosensitizer, clinically approved and used as a solvent-based formulation (Foscan<sup>®</sup>; Biolitec Research GmbH, Jena, Germany) for the treatment of head and neck cancers.<sup>7</sup> In order to improve its bioavailability and efficacy, and to reduce side effects, two liposomal forms of mTHPC were introduced: conventional liposomes (Foslip<sup>®</sup>; Biolitec Research GmbH), and polyethylene glycosylated (PEGylated) liposomes (Fospeg<sup>®</sup>; Biolitec Research GmbH). The grafting of polyethylene glycol (PEG) to the surface of liposomes serves to inhibit their recognition and uptake by the reticuloendothelial system (RES), which is a major disadvantage of conventional liposomes.<sup>3</sup>

Foslip<sup>®</sup> and Fospeg<sup>®</sup>, separately, were shown to produce a superior PDT efficacy compared to Foscan<sup>®</sup> in vitro and in vivo.<sup>8–11</sup> However, no detailed in vivo comparison of these liposomal formulations in the same model has been reported to date. The aspects of comparison of the two liposomal mTHPC forms were the tumor and plasma fluorescence kinetics in the window–chamber model in rats<sup>12</sup> and photothrombic activity in the tumor-free chick chorioallantoic membrane.<sup>13</sup> Fospeg<sup>®</sup> exhibited an earlier and higher tumor fluorescence peak compared to Foslip<sup>®</sup>,<sup>12</sup> and was shown to require a twice lower light dose to induce certain vascular damage.<sup>13</sup> The pharmacokinetic profiles of mTHPC and lipid of the liposomal formulations in rats were recently reported by Decker et al,<sup>14</sup> and the ratio of rate constants of mTHPC elimination from the bloodstream within the lipid formulation and after transfer from the liposomes to the blood components was calculated. The results of this study suggested that a fraction of mTHPC is released from liposomes prior to elimination from the blood stream.

Although progress has been made in the comprehension of the behavior of liposomal formulations of photosensitizers, the critical parameter to consider when optimizing liposomal PDT is still not clear from the studies. Successful delivery to the target requires stable retention of the drug by the nanoparticle carrier while in circulation. The rate of in vivo drug release is an extremely important, although rarely measured, parameter, as it can influence the clearance rate of the drug from the blood circulation, the bioavailability, and thus the activity of the drug at its site of action, as well as the targetability of the drug. Along with the drug release rate, blood circulation time and the spatiotemporal uptake in the tumor are considered to be the crucial properties of the liposomal drug formulation.<sup>15,16</sup>

The aim of this study was to compare and interlink the properties related to the drug behavior in vivo and the efficacy of PDT treatment with Foslip<sup>®</sup> and Fospeg<sup>®</sup> in

tumor-bearing mice. The pharmacokinetics, biodistribution, drug release, stability of liposomes, and intratumoral mTHPC localization were investigated, as well as the PDT outcome at different drug–light intervals.

## Materials and methods

### Photosensitizers

It should be noted that mTHPC and its liposomal formulation, Foslip<sup>®</sup>, were provided by Biolitec Research GmbH (Jena, Germany). Foslip<sup>®</sup> is based on dipalmitoylphosphatidylcholine (DPPC), dipalmitoylphosphatidylglycerol (DPPG), and mTHPC, with a drug:lipid ratio of 1:12 (mol/mol) and a DPPC:DPPG ratio of 9:1 (w/w). Foslip<sup>®</sup> was reconstituted from lyophilized powder in distilled water as per the manufacturer's instructions. The Fospeg<sup>®</sup> formulation (DPPC:DPPG: poly[ethylene glycol]-distearoylphosphatidylethanolamine [PEG–DSPE] = 9:1:1; 1:13 drug:lipid ratio [mol/mol]) was prepared by the filter extrusion technique as reported before.<sup>17</sup> The Z-average diameter of liposomes, as measured by dynamic light scattering on a Malvern ZetaSizer Nano (Malvern Instruments, Malvern, UK), was  $111 \pm 8$  nm (polydispersity index,  $0.113 \pm 0.01$ ) for Foslip<sup>®</sup> and  $114 \pm 7$  nm (polydispersity index,  $0.108 \pm 0.01$ ) for Fospeg<sup>®</sup>.

### Animals, tumor model, and cell culture

Animal procedures were performed in compliance with the French national guidelines and with the approval of the regional ethics committee for animal experimentation “Nancy-Lorraine – Nord-Est.” The animals received care in accordance with the established guidelines of the Federation of European Laboratory Animal Science Associations. All procedures involving animals were performed under general anesthesia with inhaled isoflurane (Forene; Abbott Laboratories, Abbott Park, IL, USA) using a Univentor 400 anesthesia unit (Genestil, Royaucourt, France), with every effort made to minimize suffering. Mice were housed in filtered air cabinets with a 12-hour light/dark cycle at 22°C–24°C and 50% humidity, provided with food and water ad libitum, and manipulated following aseptic procedures. Female NMRI<sup>nu/nu</sup> mice (Janvier, St Berthevin, France) aged 9–10 weeks were used, with a mean body weight of  $29 \pm 2$  g. Mice were inoculated subcutaneously in the left flank with  $8 \times 10^6$  exponentially growing HT29 human colon adenocarcinoma cells (ATCC; LGC Promochem, Molsheim, France), the model that was used for previous PDT experimentation.<sup>18</sup> The experiments were initiated 5–7 days after inoculation, when the tumors reached 4–5 mm in diameter. Foslip<sup>®</sup> or Fospeg<sup>®</sup> was administered intravenously

by a tail vein injection at a dose of 0.15 mg/kg of mTHPC. Following the injection, mice were kept in the dark and experiments were undertaken with minimal ambient light.

HT29 cells used for tumor inoculation were maintained in phenol red-free Roswell Park Memorial Institute 1640 medium (Invitrogen) supplemented with 9% (vol/vol) heat-inactivated fetal calf serum, penicillin (10,000 IU), streptomycin (10,000 µg/mL), and 1% (vol/vol) 0.1 M glutamine (Life Technologies, Carlsbad, CA, USA). Cells were kept as a monolayer culture in a humidified incubator (5% CO<sub>2</sub>) at 37°C. Cell culture was reseeded every week to ensure exponential growth.

## Blood sample preparation

At predetermined times after intravenous photosensitizer injection, 500 µL of blood was drawn by cardiac puncture and placed in heparin-coated Vacutainer® blood collection tubes (BD Diagnostics, Le Pont de Claix Cedex, France). The blood was kept at 4°C and centrifuged for 15 minutes at 1,200 g before sample plasma analysis by high-performance liquid chromatography and photoinduced fluorescence quenching techniques.

## Pharmacokinetics and biodistribution

Tumor-bearing mice (4–6 per group) were sacrificed at predetermined time points after the liposomal mTHPC injection. Tissue samples included in the analysis were tumor, skin, muscle, spleen, liver, kidneys, heart, lungs, and plasma. Tissue samples were rinsed thrice in 0.9% NaCl and kept at –80°C prior to analysis. The mTHPC concentration in the samples was determined by high-performance liquid chromatography, as previously described.<sup>19</sup> The plasma pharmacokinetics were analyzed using compartmental and noncompartmental methods.<sup>20</sup> Elimination rate constants from the tissues were calculated from semi-logarithmic plots of the three last data points (15 hours, 24 hours, and 48 hours).

## mTHPC release from liposomes

The release of mTHPC from liposomes during the circulation in blood was estimated using the technique of photoinduced fluorescence quenching.<sup>21</sup> It consists in a significant liposomal mTHPC fluorescence decrease after irradiation of the sample with a very low light dose, which is restored after the destruction of liposomes by a neutral detergent. The mechanism of fluorescence quenching is related to the formation of a small amount of quenchers upon photoirradiation, which are primary nonfluorescent photooxidation products of mTHPC.<sup>21</sup> The effect of photoinduced fluorescence

quenching arises from energy migration between closely located mTHPC molecules in liposomes, the energy being dissipated by nonfluorescent photoproducts acting as energy traps. After addition of the detergent, the energy migration ceases, and the mTHPC fluorescence of the sample is restored. The amplitude of the effect is significantly dependent on the mTHPC concentration in liposomes.<sup>17</sup>

As described,<sup>17</sup> the amplitude of photoinduced fluorescence quenching in the plasma samples allows the local mTHPC concentration in liposomes to be determined using a method described in Table S1. These data are used to calculate the percentage of the drug released from intact liposomes at a given time after injection when compared to the initial drug formulation (Foslip® or Fospeg®).

Samples of plasma containing mTHPC were irradiated by a 20 mW 650 nm laser (Global Laser Limited, Gwent, UK) for 30 seconds under continuous stirring at 21°C. Fluorescence spectra were recorded on a PerkinElmer LS55B spectrofluorimeter (PerkinElmer, Waltham, MA, USA).

## Liposome destruction in mouse serum

Liposome destruction upon incubation in diluted mouse serum was estimated by Nanoparticle Tracking Analysis,<sup>22</sup> using a NanoSight LM20 (NanoSight, Ltd, Amesbury, UK) equipped with a 640 nm, 40 mW laser, as previously described.<sup>23</sup> Blood was drawn from the mice and precipitated in Vacutainer® SST™ II Advance tubes (BD Diagnostics) to obtain serum (pooled from five mice). Foslip® and Fospeg® (mTHPC concentration of  $2.0 \times 10^{-5}$  M), and 20% filtered serum were incubated in phosphate buffered saline at 37°C for up to 24 hours. Aliquots were diluted 250× in phosphate buffered saline and analyzed by the NanoSight system (NanoSight, Ltd). Samples were injected into the viewing chamber, and the particles moving under Brownian motion were visualized, with the videos recorded at 30 frames/second for 40 seconds with fixed shutter and gain adjustments. At least 1,200 tracks were completed during the video data analysis using Nanoparticle Tracking Analysis version 2.3 software (NanoSight, Ltd). Three different samples were used for each formulation, and each aliquot was run in quadruplicate. No Fospeg® aggregation was registered in serum, while the Foslip® peak diameter increased by 30 nm after 24 hours.

## Fluorescence confocal microscopy in live animals

Measurements of intratumoral mTHPC localization in whole tumor in live mice were performed using fluorescence multiphoton confocal microscopy. Twelve days after tumor

cell inoculation, when the tumors reached a diameter of 7–8 mm with clearly visible vessels under the white-light microscope, which allowed for exact and clear identification under the fluorescent microscope, the animals were injected with 7.5 mg/kg of mTHPC as Foslip® or Fospeg®. Measurements were performed at 3 hours, 6 hours, 15 hours, and 24 hours postinjection. Three to four mice were used for each time point.

Twenty minutes prior to macroscopy observations, mice were anesthetized with an intraperitoneal injection of a ketamine/xylazine mixture. The vascular tumor compartment was stained as described earlier.<sup>16</sup> Briefly, 5 minutes prior to macroscopy observations, 40  $\mu$ L of 0.2  $\mu$ m of fluorescent carboxylate-modified polystyrene microspheres (F-8809; Molecular Probes®; Life Technologies) was injected, rendering perfused vessels highly fluorescent. An incision of the skin in the vicinity of the tumor was made without damaging the blood vessels. The skin with the subcutaneous tumor and surrounding blood vessels was detached from underlying tissues, turned inside-out, and fixed on a flat soft support in order to expose the tumor while preserving blood circulation.

Tumors were visualized using a custom-built two-photon scanning microscope (Leica SP5 coupled to a Leica Z16 Apo microscope head; Leica Microsystems, Wetzlar, Germany), coupled to a Ti:sapphire laser (Mira Optima 900F X-Wave; Coherent, Inc, Santa Clara, CA, USA), mode locked at 706 nm with a pulse duration <200 fs at the sample.<sup>24</sup> Fluorescence emission of mTHPC (peak 652 nm) was collected from 630–670 nm on one channel, and fluorescence from the microspheres (peak 560 nm) was collected from 540–590 nm on a second channel, with the pinhole locked at 600  $\mu$ m. An Apo 2  $\times$  dry objective (working distance 39 mm) was used to capture each image of 512  $\times$  512 pixels. The fluorescence images shown in the article are the max projections from a three-dimensional image stack (50–60 images; line average 4) along the orthogonal axis (z-height 2.5–4.5 mm). No visible photobleaching was observed during image acquisition. In control mice (no drug, no vessel marker), no significant tumor autofluorescence was detected at selected parameters. White-light images of the tumors were obtained with a Leica MacroFluo™ Z16 Apo microscope (Leica Microsystems) using 1  $\times$  Apo objective (working distance 97 mm), zoom factor 0.5, and exposure 200 ms.

A quantitative analysis of the colocalization of mTHPC and the vessel marker was performed using the colocalization tool in the Leica Application Suite – Advanced Fluorescence v.2.7 software (Leica Microsystems) with 20% background

subtraction and 30% threshold for both channels. Three adjacent images from the three-dimensional stack were merged into max projection with no signal saturation. Three different projections were used for each tumor, and three regions of interest, 1,300  $\mu$ m  $\times$  1,300  $\mu$ m each, with blood vessels and surrounding tumor tissue, were selected for each projection. The selection was based on the sufficient fluorescent microspheres signal delineating the blood vessels. Colocalization was defined as co-compartmentalization of mTHPC and fluorescent microspheres in tumor blood vessels. Colocalization was quantified with Pearson's correlation coefficient (PCC). Absolute PCC values of 1–0.7 indicate a relatively strong correlation, 0.69–0.36 indicate a moderate correlation, 0.35–0.2 indicate a weak correlation, and <0.2 indicates the absence of a correlation.<sup>25,26</sup> The square of PCC represents the percentage of mTHPC fluorescence signal predictable from the signal of the vessel marker.<sup>25</sup>

## Photodynamic treatment and assessment of PDT efficacy

Tumor irradiation was performed at 652 nm with a Ceralas PDT diode laser (CeramOptec GmbH, Bonn, Germany) at a fluence of 10 J cm<sup>-2</sup> and a fluence rate of 30 mW cm<sup>-2</sup>. Four DLIs were used (3 hours, 6 hours, 15 hours, and 24 hours), with 5–9 mice per group. Five mice were randomly selected as the control group (no drug, no light). Mice were kept in the dark for 4 days after PDT. Three times per week, the perpendicular diameters of the tumors were measured to document tumor growth. Tumor volume (*V*) was calculated using the equation

$$V = W^2 \times Y/2, \quad (1)$$

where *W* and *Y* are the smaller and larger diameters. No sign of tumor recurrence at 120 days post-PDT was qualified as a cure. Cured animals were not included, either in the graphical representation or in the calculations of the time to reach 10 $\times$  initial tumor volume. A small number of mice with tumor recurrences, but with tumor regrowth halted at 1–7 $\times$  the initial tumor volume for up to 120 days post-PDT, were censored.

## Statistics

Statistical analysis of tumor response between PDT groups was carried out using the log-rank test. All other data were analyzed using the nonparametric Mann–Whitney *U*-test with a significance level of *P* < 0.05. StatView v.5.0 (SAS Institute Inc, Cary, NC, USA) was used for calculations. All results are presented as the mean  $\pm$  standard deviation.

## Results

### Plasma pharmacokinetics of Foslip<sup>®</sup> and Fospeg<sup>®</sup>

The pharmacokinetic profiles of mTHPC injected as Foslip<sup>®</sup> and Fospeg<sup>®</sup> in tumor-bearing mice are shown in Figure 1. Fospeg<sup>®</sup> exhibited significantly higher drug levels for the first 6 hours, with similar profiles for both mTHPC formulations afterwards. The profiles followed a multiexponential decay, and the pharmacokinetic parameters were calculated using compartmental and noncompartmental approaches (Table 1). For the former, the data best fit a three-exponential decay, with significant differences between Foslip<sup>®</sup> and Fospeg<sup>®</sup> in the half-lives of the first and second compartments, and a similar third compartment half-life. The experimental time points used were long enough to detect a third half-life observed in other studies.<sup>11,19</sup> The initial volume of distribution of Fospeg<sup>®</sup> was seven times lower than that of Foslip<sup>®</sup>. The volume of distribution calculated by the noncompartmental method was lower for Fospeg<sup>®</sup>.

### Release of mTHPC from liposomes

The calculation of the mTHPC amount released from the liposomes in the blood circulation is shown in Table S1, and the measurement of photoinduced fluorescence-quenching amplitude in the plasma samples of Foslip<sup>®</sup> and Fospeg<sup>®</sup> injected in mice, are shown in Figure S5. Both formulations exhibited a significant release of mTHPC in the blood circulation (Figure 2). The efflux from Foslip<sup>®</sup> proceeded much faster as compared to Fospeg<sup>®</sup>: already 1 hour postinjection, more than 70% of mTHPC was released from Foslip<sup>®</sup> that remained in the circulation, as compared to 40% release from

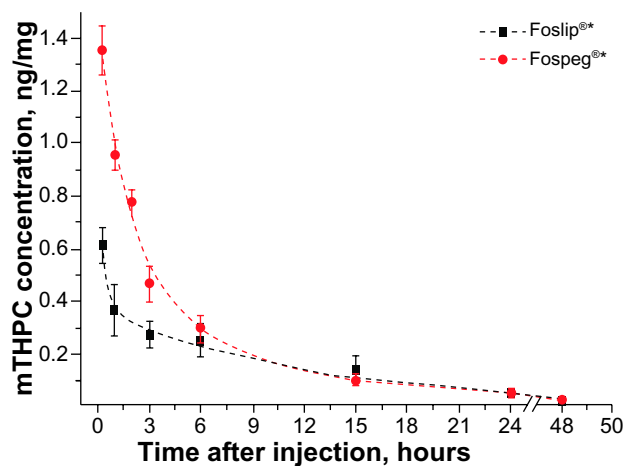


**Figure 1** The mTHPC concentration in plasma after injection of 0.15 mg/kg of mTHPC as Foslip<sup>®</sup> or Fospeg<sup>®</sup> into tumor-bearing mice.

**Note:** The data are fitted to a three-compartmental model. \*Biolitec Research GmbH, Jena, Germany.

**Abbreviation:** mTHPC, meta-tetra(hydroxyphenyl)chlorin.

**Table 1** Pharmacokinetic parameters of mTHPC after injection with Foslip<sup>®</sup> or Fospeg<sup>®</sup>\*

Pharmacokinetic parameter	Foslip <sup>®</sup>	Fospeg <sup>®</sup>
<b>Three-compartmental model</b>		
Initial dosage, mg/kg	0.15	0.15
Initial concentration, $\mu\text{g/mL}$	0.79	5.57
Initial volume of distribution, mL/kg	189.9	26.9
Half-life ( $t_{1/2}$ ) of the first compartment, 1/hour	0.029	0.061
Half-life ( $t_{1/2}$ ) of the second compartment, 1/hour	0.71	2.49
Half-life ( $t_{1/2}$ ) of the third compartment, 1/hour	18.0	18.1
<b>Noncompartmental model</b>		
Plasma clearance, mL/(kg · hour)	28.9	22.9
Mean residence time, hour	16.4	11.3
Volume of distribution ( $V_d$ ), mL/kg	472.0	259.4
Half-life ( $t_{1/2}$ ), 1/hour	11.0	8.3
Elimination rate constant ( $K_{el}$ ), 1/hour	0.063	0.084

**Note:** \*Biolitec Research GmbH, Jena, Germany

**Abbreviation:** mTHPC, meta-tetra(hydroxyphenyl)chlorin.

Fospeg<sup>®</sup> (Figure 2, inset). The mTHPC release from Foslip<sup>®</sup> reached the plateau after 2 hours, leaving <15% of mTHPC in the liposomes. In contrast, mTHPC redistribution from Fospeg<sup>®</sup> proceeded until 6 hours postinjection, with 30% of the mTHPC present in the circulation in the liposomal form at that time. After 24 hours, only 6% of the mTHPC was further released.

### Destruction of mTHPC liposomal formulations in mouse serum

The stability of liposomal formulations of mTHPC in serum in vitro is shown in Figure 3A. Foslip<sup>®</sup> exhibited a destruction of 20% of liposomes during the first 5 minutes of incubation, followed by a gradual destruction of another 40% after 6 hours. Fospeg<sup>®</sup> showed a behavior qualitatively different

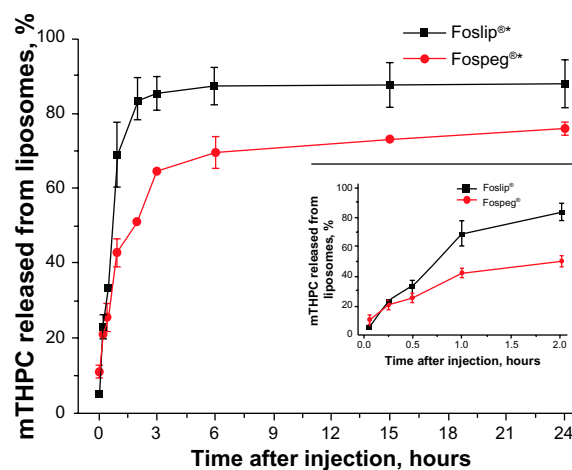


**Figure 2** Release of mTHPC from Foslip<sup>®</sup> and Fospeg<sup>®</sup> in the blood circulation after injection into tumor-bearing mice.

**Note:** In the insert, the zoomed 0–2-hour region is shown. \*Biolitec Research GmbH, Jena, Germany.

**Abbreviation:** mTHPC, meta-tetra(hydroxyphenyl)chlorin.

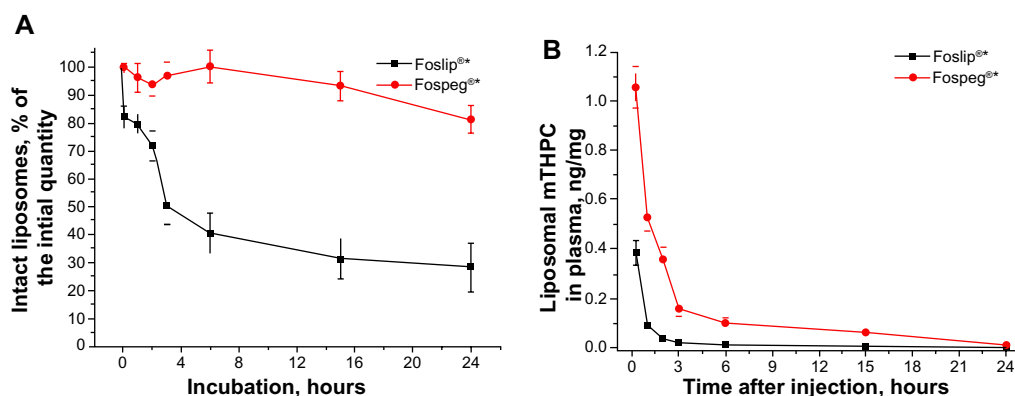


**Figure 3** Kinetics of mTHPC-loaded liposome destruction in mouse serum, and amount of liposomal mTHPC in plasma.

**Notes:** (A) Kinetics of mTHPC-loaded liposome destruction in mouse serum, as determined by NTA. (B) Amount of liposomal mTHPC in plasma, calculated from the data presented in Figures 1, 2, and 3A as (plasma mTHPC concentration) · (% of mTHPC in liposomes) · (% of intact liposomes). \*Biolitec Research GmbH, Jena, Germany.

**Abbreviations:** mTHPC, meta-tetra(hydroxyphenyl)chlorin; NTA, Nanoparticle Tracking Analysis.

from that of Foslip®: liposomes remained stable up to 6 hours of incubation in serum, and less than 20% were destroyed after 24 hours of incubation. Assuming that the stability of liposomes in serum corresponds to that in the blood circulation, the amount of liposomal mTHPC in plasma may be estimated by combining the results in Figure 3A with the plasma pharmacokinetics (Figure 1) and the mTHPC release from liposomes in the circulation (Figure 2). This estimation is shown in Figure 3B. Fospeg® provides a significant quantity of liposomal mTHPC up to 15 hours postinjection. In contrast, Foslip®-injected mTHPC is present in the liposomal form only for the first hour.

### Biodistribution of Foslip® and Fospeg®

The mTHPC levels in selected tissues after injection of Foslip® or Fospeg® are shown in Figure 4. The drug concentration in the tumor reaches a plateau significantly earlier with Fospeg® (6 hours) than with Foslip® (15 hours) (Figure 4A).

Already 2 hours after injection, the mTHPC level in the tumor is three times higher for Fospeg®. Accumulation in skin follows the same profile as in the tumor, but with much lower drug levels (Figure 4A). Muscle accumulates the smallest amount of mTHPC of all the studied tissues, with the Fospeg®-injected drug level being slightly lower than that of Foslip®. The tumor/muscle ratio reaches the maximal values of about 10 at 6 hours for Fospeg®, while Foslip® displays a similar maximum at 15 hours (Figure S1A).

The highest mTHPC levels were found in the spleen and liver for both formulations (Figure 4B). The spleen uptake of Foslip®-injected mTHPC peaks at 1 hour, and is more than twice as high as that of Fospeg®, which reaches a maximum after 6 hours. The liver shows similar kinetic profiles for both formulations, peaking at 3 hours, although the levels for Fospeg® are lower. The kidney level of Fospeg®-injected mTHPC showed a very high drug peak at 3 hours, which is in contrast to the Foslip® profile, where the mTHPC level

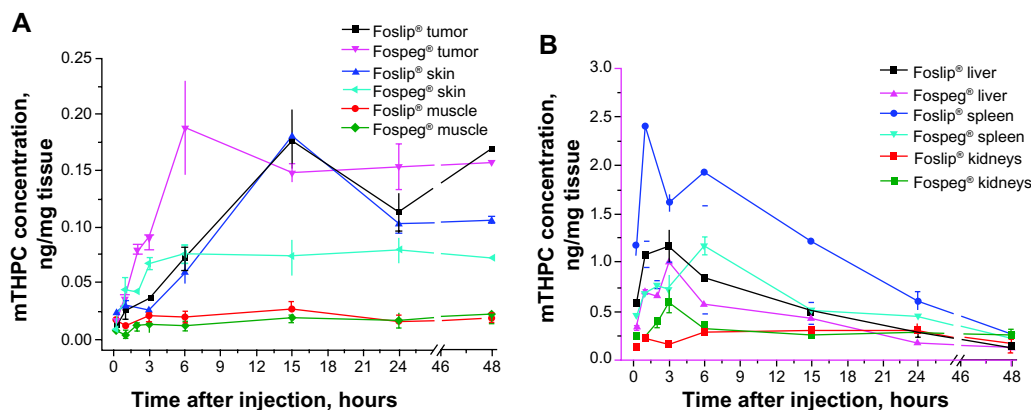


**Figure 4** Concentration of mTHPC in selected tissues as a function of time following injection of Foslip® or Fospeg®.

**Notes:** (A) tumor, skin, and muscle; (B) spleen, liver, and kidneys. \*Biolitec Research GmbH, Jena, Germany.

**Abbreviation:** mTHPC, meta-tetra(hydroxyphenyl)chlorin.

**Table 2** Rate constants of the terminal phase of mTHPC elimination from tissues

Tissue	Foslip®*	Fospeg®*
	<b>Elimination rate constant, <math>\times 10^3 \text{ h}^{-1}</math></b>	
Tumor	0.56	0.69
Plasma	18.4	18.2
Liver	17.7	14.7
Spleen	19.1	12.1
Kidneys	9.61	0.14
Lungs	9.07	7.84
Heart	4.62	3.72
Skin	5.54	0.54

**Note:** \*Biolitec Research GmbH, Jena, Germany.

**Abbreviation:** mTHPC, meta-tetra(hydroxyphenyl)chlorin.

peaked at 6 hours (Figure 4B). After 6 hours, the drug levels for both formulations were similar. In the lungs, the Fospeg®-injected drug level peaked at 3 hours, while Foslip®-injected mTHPC peaked at 6 hours (Figure S1B). No differences were found in terms of the accumulation in the heart (Figure S1B).

The terminal mTHPC elimination rate constants were similar for the plasma, liver, and spleen, indicating that they are part of one compartment for elimination, both for the Foslip®- and the Fospeg®-injected drug (Table 2). mTHPC levels in the tumor are fairly constant for up to 48 hours for both formulations. In contrast to Foslip® with its relatively fast elimination from the kidneys, Fospeg®-injected mTHPC – in addition to its high retention in that organ – is eliminated extremely slowly. Additionally, the diffusion of Fospeg®-injected mTHPC from the skin is very slow, while Foslip® shows a significant elimination rate. Elimination rates from the lungs and heart were similar for both formulations.

### Intratumoral localization of liposomal mTHPC in vivo

Figure 5 shows the intratumoral distribution of Fospeg®-injected mTHPC with regard to the tumor vasculature obtained 3–24 hours postinjection. After 3 hours, mTHPC

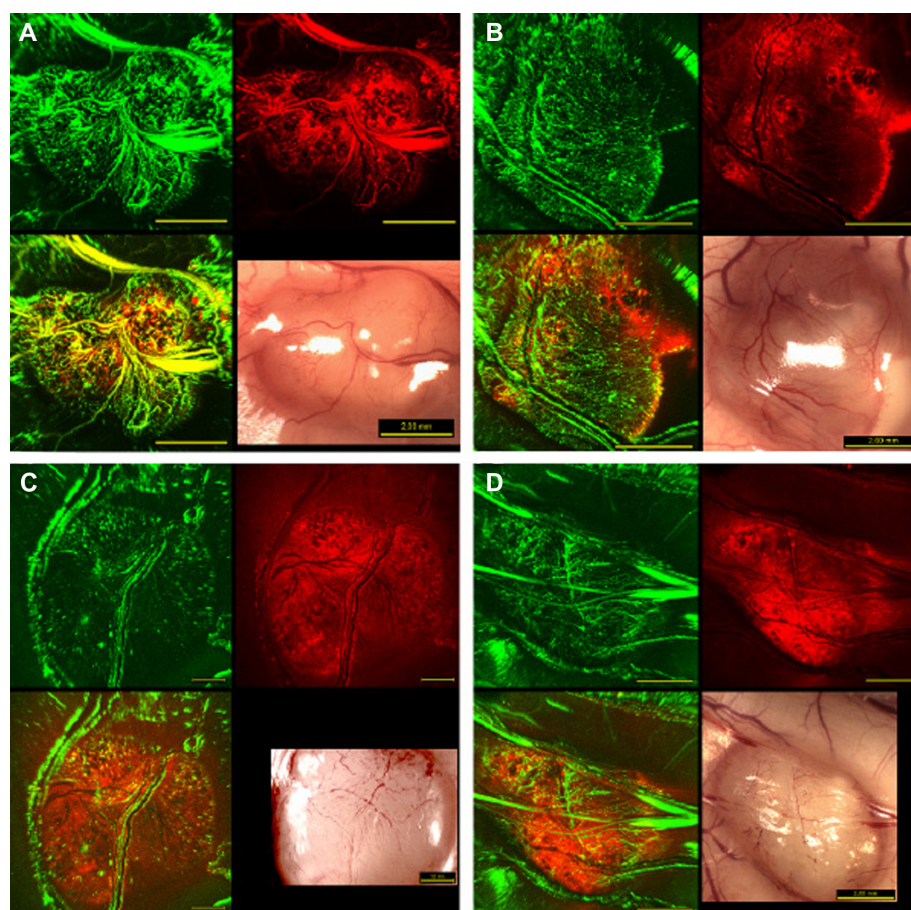


**Figure 5** Representative in vivo multiphoton confocal and white-light macroscopy images of whole HT29 tumors.

**Notes:** Images were acquired (A) 3 hours, (B) 6 hours, (C) 15 hours, and (D) 24 hours following injection of 7.5 mg/kg of mTHPC in the form of Fospeg® (Biolitec Research GmbH, Jena, Germany). Vascular perfusion marker fluorescence is shown in green false color, and mTHPC fluorescence in red. The lower left-hand image of each block is the overlay of the green and red channels. The scale bar values shown on the white-light images apply to all four images in each four-image block.

**Abbreviation:** mTHPC, meta-tetra(hydroxyphenyl)chlorin.

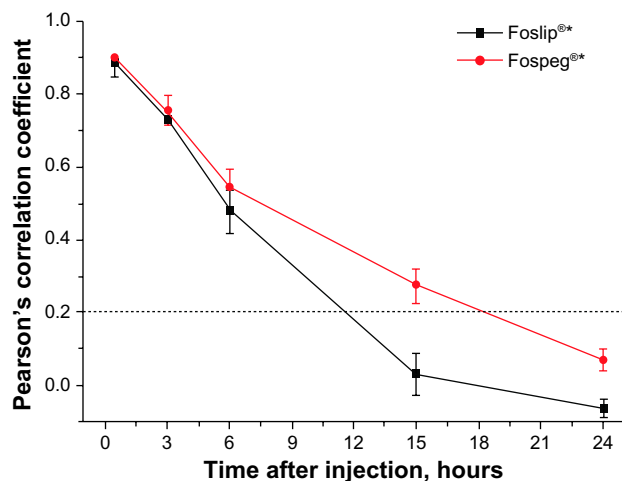


**Figure 6** Pearson's correlation coefficient values quantifying the colocalization of the vessel perfusion marker and liposome-injected mTHPC in the HT29 tumor.

**Note:** The dotted line indicates the absence of a correlation below. \*Biolitec Research GmbH, Jena, Germany.

**Abbreviation:** mTHPC, meta-tetra(hydroxyphenyl)chlorin.

was visibly retained in or near the blood vessels, showing overlap of the two colors (Figure 5A). At 6 hours, mTHPC diffused to the tumor tissue close to the vasculature, with the fluorescence signal having dropped farther into the tumor tissue, and was also present in smaller blood vessels and vessel walls (Figure 5B). By 15 hours, mTHPC fluorescence arose mainly from the tumor tissue (Figure 5C) at all distances to tumor vessels, with a small overlap with the vessel marker. At 24 hours, mTHPC fluorescence was detected throughout the tumor tissue, without any visible contribution from the vessels (Figure 5D). Foslip<sup>®</sup> presents a similar pattern of distribution (Figure S2), with the exception of 15 hours, where no signal overlap with the perfusion marker was visible.

In order to quantify the colocalization of Foslip<sup>®</sup>- and Fospeg<sup>®</sup>-injected mTHPC, as well as with the vessel

marker, we calculated the PCC (shown in Figure 6). At 0.5 hours postinjection, both formulations showed a very high correlation with the vessel marker (for the confocal image acquired at 30 minutes, see Figure S3). High PCC values were obtained at 3 hours, indicating that mTHPC was predominantly localized in blood vessels, with a smaller part diffused to the tumor tissue. By 6 hours, significantly lower PCC values were obtained. PCC<sup>2</sup> values indicated that 30% and 23% of the mTHPC signal was predictable from the vessel marker signal for Fospeg<sup>®</sup> and Foslip<sup>®</sup>, respectively. At 15 hours, Foslip<sup>®</sup> displayed the absence of a correlation, while Fospeg<sup>®</sup> showed a weak correlation with a PCC<sup>2</sup> value of 8%. At 24 hours, both formulations showed no correlation with the marker, indicating that mTHPC was distributed in the tissue compartment alone.

### Efficacy of PDT treatment

Kaplan–Meier plots of tumor response to Foslip<sup>®</sup>- and Fospeg<sup>®</sup>-PDT are presented in Figure 7A and B. Mean tumor growth time is shown in Table 3. Tumor response to Foslip<sup>®</sup>-PDT was maximal at DLIs of 15 hours and 24 hours, which was significantly higher than at 3 hours and 6 hours ( $P < 0.01$ ). PDT at 3 hours was ineffective, with no statistical difference observed from the control group (Figure 7A). Fospeg<sup>®</sup> showed the highest PDT efficacy at a DLI of 15 hours compared to the other three DLIs ( $P < 0.01$ ), with a tumor growth delay of 54.8 days. There was no statistical difference in tumor response with Fospeg<sup>®</sup>-PDT at all other DLIs (Figure 7B) ( $P > 0.2$ ), although the response was significantly different in the control group ( $P < 0.005$ ). Except for 24 hours ( $P > 0.2$ ), Fospeg<sup>®</sup>-PDT was more effective than Foslip<sup>®</sup> treatment at all other DLIs ( $P < 0.03$ ). It is noteworthy that treatment with Fospeg<sup>®</sup>

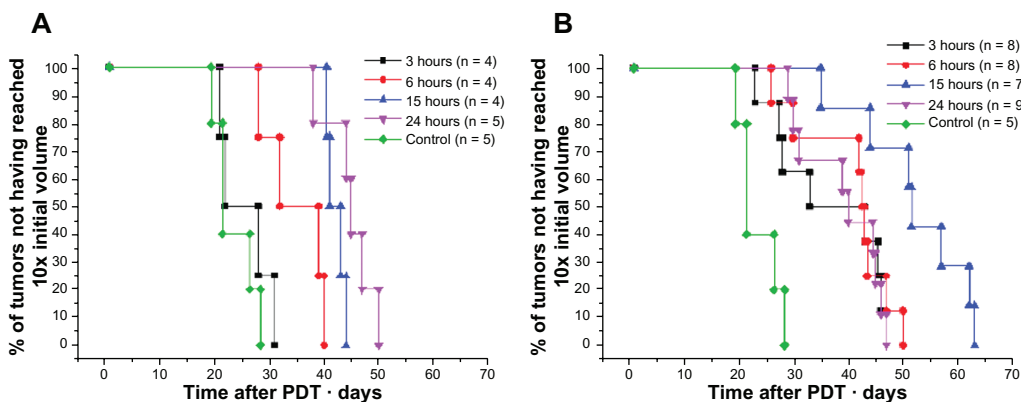


**Figure 7** Kaplan–Meier plots of HT29 tumor growth delay after PDT with Foslip<sup>®</sup> and Fospeg<sup>®</sup> at different DLIs.

**Notes:** (A) Foslip<sup>®</sup> and (B) Fospeg<sup>®</sup>. Cured mice are neither shown nor included in the calculations. \*Biolitec Research GmbH, Jena, Germany.

**Abbreviations:** n, number; PDT, photodynamic therapy; DLI, drug–light interval.



**Table 3** Mean tumor growth time (time to reach 10 × the initial tumor volume) after Foslip® and Fospeg®-PDT, and cured and censored mice

DLI	Foslip®		Fospeg®	
	Growth time, days	Cured <sup>a</sup> (censored <sup>b</sup> ) mice	Growth time, days	Cured <sup>a</sup> (censored <sup>b</sup> ) mice
3 hours	25.5 ± 5.0 <sup>c</sup>	1 (2)	38.9 ± 9.4	0 (2)
6 hours	34.8 ± 5.7 <sup>c</sup>	1 (1)	42.6 ± 6.3	1 (1)
15 hours	42.1 ± 1.7 <sup>c,d</sup>	1 (1)	54.8 ± 7.5 <sup>e</sup>	1 (1)
24 hours	44.4 ± 4.5 <sup>d</sup>	0 (0)	38.8 ± 7.3	0 (0)
Control	22.7 ± 4.0, 0(0)			

**Notes:** <sup>a</sup>Cure was defined as the absence of tumor recurrence at 120 days post-PDT; <sup>b</sup>censored mice exhibited recurrences with tumor regrowth halted at 1–7 × the initial tumor volume; <sup>c</sup>statistically different from Fospeg® at the same DLI,  $P < 0.05$ ; <sup>d</sup>statistically different from Foslip® at DLI 3 hours and 6 hours,  $P < 0.02$ ; <sup>e</sup>statistically different from Fospeg® at DLI 3 hours, 6 hours, and 24 hours,  $P < 0.01$ . \*Biolitec Research GmbH, Jena, Germany.

**Abbreviations:** PDT, photodynamic therapy; DLI, drug–light interval.

at DLI of 3 hours showed an efficacy similar to that of the treatment with Foslip® at 15 hours. In a small number of animals, a permanent tumor remission was observed.

## Discussion

### Pharmacokinetics and drug release

Pharmacokinetic data indicate a higher confinement of Fospeg®-injected mTHPC to vasculature, as well as much higher drug levels compared to Foslip® (Table 1 and Figure 1). The release rate of the liposome-encapsulated drug in circulation is an essential parameter affecting the pharmacokinetics and therapeutic efficacy of the formulation.<sup>15,27</sup> Although in vitro liposomal mTHPC release to serum proteins has been reported,<sup>17</sup> this characteristic was not studied in vivo in sufficient detail. The results of the pharmacokinetic study by Decker et al<sup>14</sup> suggested that a fraction of mTHPC is released from liposomes prior to elimination from the blood stream, as deduced from the ratio of rate constants of mTHPC elimination from the blood stream within the lipid formulation and after transfer from the liposomes to the blood components. Both Foslip® and Fospeg® show major efflux of mTHPC from liposomes in the blood circulation (Figure 2). Due to both the release and liposome destruction, Foslip® pharmacokinetics after 1 hour already reflect the circulation of free-mTHPC released from the liposomes (Figure 3B). Fospeg® exhibits a slower release rate due to PEG steric protection,<sup>3</sup> with a significantly higher amount of mTHPC remaining in the liposomes, and the absence of carrier destruction (Figure 3A). For the first 6 hours the pharmacokinetics of Fospeg® in the blood is a combination of the free and liposomal forms of the drug. The differences in  $t_{1/2}$  of the first and second pharmacokinetic compartments of Foslip® and Fospeg® (Table 1) correlate well with the release rate from both formulations and the destruction of conventional liposomes. The identical  $t_{1/2}$  of the third compartment indicates that most of mTHPC from

both formulations is in the nonliposomal form (Figure 2). The significant release of mTHPC from Fospeg® explains the similarity in the terminal phase elimination rate constants reported for Foscan® and Fospeg®.<sup>11</sup>

The decrease in the release rate of mTHPC from Fospeg® after 3 hours (Figure 2) is explained by the difference in the physical state of the liposomes as a function of the drug content. Indeed, with liposomal drug loads ranging from 8 mol% (initial drug load of Fospeg®) to 3 mol% (corresponds to a 65% mTHPC release from Fospeg®), the lipid bilayer is in a liquid–crystalline state,<sup>28</sup> which facilitates the release.<sup>17,29</sup> At lower drug loads of <3 mol%, the lipid bilayer is in the gel state,<sup>28</sup> which slows down the release.

Improved plasma stability of the liposomes has been found to correlate with increased drug delivery to tumors.<sup>30</sup> The simulation of pharmacokinetic disposition of nonreleased liposomal mTHPC is presented on Figure 3B. Although the estimation of liposome stability was carried out in serum in vitro (not in vivo), a direct correlation between the stability in vitro and in vivo had been established before.<sup>31,32</sup> Liposomal mTHPC injected as Foslip® is almost completely eliminated from the circulation already after 1 hour, while Fospeg® provides a substantial amount of circulating liposomal drug for up to 6 hours (Figure 3B).

Despite the fast elimination of conventional liposomal mTHPC from circulation, its advantage compared to solvent-based Foscan® is that it releases the drug to lipoproteins in the photoactive monomer form.<sup>23</sup> Fospeg® evidently provides monomerization of the released mTHPC plus the prolonged circulation of its liposomal form.

### Biodistribution

The prolonged blood circulation of liposomal mTHPC injected as Fospeg® serves as a basis for rapid mTHPC accumulation in the tumor by means of the EPR effect. The

EPR effect consists in the extravasation of nanocarriers into the tumor tissue from the leaky tumor vessels and prolonged retention in the tissue due to impaired lymphatic drainage.<sup>33</sup> Being a progressive phenomenon, it requires multiple passages of the liposomal drug through the tumor vessels in order to achieve a substantial level of accumulation in the tumor.<sup>33</sup> Apparently, efficient EPR-based accumulation cannot be achieved with Foslip<sup>®</sup> (Figure 3B).

As anticipated, Fospeg<sup>®</sup> reaches the maximal accumulation in the tumor much earlier than Foslip<sup>®</sup> (6 hours versus 15 hours; Figure 4A). Similar peak times were found for Fospeg<sup>®</sup> in a tumor-grafted rat model<sup>11</sup> and in feline patients.<sup>9</sup> It is noteworthy that the maximal level of mTHPC accumulation in the tumor is practically the same for Foslip<sup>®</sup> and Fospeg<sup>®</sup> (Figure 4A), although a higher accumulation of long-circulating liposomes could be expected.<sup>34</sup> This could be explained by the insufficient liposomal drug concentration in plasma after 6 hours (Figure 3B) to increase the tumor uptake by EPR versus the drug in the nonliposomal form.

Fospeg<sup>®</sup> showed lower drug levels in the skin compared to Foslip<sup>®</sup> (Figure 4A), thus indicating that the side effects with Fospeg<sup>®</sup>-PDT may be less severe. The highest drug accumulation was observed in the liver and the spleen (Figure 4B), as described previously.<sup>11,19</sup> While conventional liposomes are rapidly uptaken in the liver and the spleen, Fospeg<sup>®</sup> shows a peak after 3–6 hours, correlating with multiple passages and the gradual accumulation of PEGylated liposomes in the RES. The elimination rates of mTHPC from RES organs are similar for Foslip<sup>®</sup> and Fospeg<sup>®</sup> (Table 2), as mTHPC is in the nonliposomal form in both cases. The cause of the significantly higher Fospeg<sup>®</sup> retention in the kidneys for the first 3 hours (Figure 4B) is unclear. A similar effect was observed for PEGylated polymer particles compared to the non-PEGylated counterpart.<sup>35</sup> Separate measurements of mTHPC and lipid content may help to elaborate upon the comparison of the behavior of both conventional and PEGylated liposomal formulations in organs, which was beyond the scope of the study.

### Intratumoral drug distribution

PDT efficacy depends not only on the bulk concentration of the photosensitizer in the tumor, but also on its spatial intratumoral localization. Drug localization near the vessel walls will favor damage and shutdown of the tumor vasculature, while localization far from the vessels will cause direct tumor cell destruction.<sup>36</sup> In vivo multiphoton microscopy applied here offers the advantages of noninvasive imaging of the whole tumor, thus providing a representation of

drug distribution with minimal perturbation. Foslip<sup>®</sup>- and Fospeg<sup>®</sup>-injected mTHPC is transported from the tumor blood vessels across the vessel walls to the tumor cells in a 3–24-hour interval (Figure 5). The diffusion to the tumor tissue is evident after 3 hours (Figure 5A), but most of the drug is localized in the vessels (Figure 6). By 6 hours, a larger part of Foslip<sup>®</sup>- and Fospeg<sup>®</sup>-injected mTHPC is in the tumor parenchyma compared to the perfused vessels (Figure 6), but it still resides not far from the tumor vasculature (Figure 5B). The shallow diffusion into the tumor tissue is likely to be the result of a high interstitial fluid pressure in the tumor.<sup>37</sup> At 15 hours, the Fospeg<sup>®</sup>-injected drug is still present in the tumor vessels (Figure 6), correlating with the prolonged blood circulation of liposomal mTHPC (Figure 3B), while Foslip<sup>®</sup> is absent in the tumor vessels. The Foslip<sup>®</sup> distribution pattern reported here corresponds to earlier results of the microscopic study.<sup>19</sup>

### Photodynamic treatment

The effect of DLI on the outcome of Fospeg<sup>®</sup>-PDT had not been reported before, as the previous studies used only a single DLI.<sup>9–11</sup> It appears from our study that irrespective of the formulation, and at identical mTHPC concentrations in the tumor, the PDT efficacy is identical (Figure 4 and Table 3). An exception here is at 15 hours DLI, where Fospeg<sup>®</sup> appears to be much more effective compared to Foslip<sup>®</sup>. This can be attributed to the intratumoral localization of mTHPC where, according to Figure 5, the drug is localized in both vascular/perivascular structures and throughout the tumor parenchyma. The importance of the intratumoral distribution for PDT efficacy has already been reported in several studies.<sup>19,38</sup>

Concerning Fospeg<sup>®</sup>, a discrepancy can be noted between the 3-hour and 6-hour DLIs, where a twice higher mTHPC concentration in the tumor does not induce better efficacy (Figures 4 and 7). With regard to drug release in plasma (Figure 2), and assuming that a comparable release pattern is observed in the tumor tissue, this apparent contradiction can be explained by the very slow release of mTHPC from the liposomal structure after 3 hours, with comparable levels of released drug after 3 hours and 6 hours. As a large amount of mTHPC will still be retained in the liposomes, and since PEGylated liposomes are known to be inefficiently uptaken by the cells, liposomal mTHPC will not, therefore, create cytotoxic reactions. Furthermore, even if singlet oxygen from liposomal mTHPC could reach vital cellular structures, mTHPC residing in the liposomes is unable to effectively generate singlet oxygen when the release from Fospeg<sup>®</sup> is less than 80% (Figure S4).

## Conclusion

This study shows the correlation between a set of parameters not reported before in one model – the drug pharmacokinetics, release properties, liposome stability, tumor uptake, and intratumoral distribution (on the one hand), and the efficacy of PDT treatment at different DLIs of two different liposomal formulations of mTHPC (on the other hand).

Characterization of the drug release and liposome stability described in the present study is an important addition to bulk plasma pharmacokinetics and tumor uptake measurements. A new method of drug release estimation used in the study was shown to be applicable for ex vivo measurements, which is important for further research in mTHPC–PDT. Both Foslip® and Fospeg® show a major efflux of mTHPC from liposomes in the circulation. Liposomal mTHPC injected as Foslip® is soon eliminated from the circulation due to drug release and liposome destruction, while Fospeg® provides a significant amount of blood-circulating liposomal mTHPC for up to 6 hours, with liposomes remaining intact. The ability of liposomes to carry the photosensitizer to the tumor and release it in the target tissue is a major factor in drug efficacy, and a prolonged blood circulation of Fospeg®–mTHPC allows for the rapid accumulation of liposomal mTHPC in the tumor by means of the EPR effect. The efficacy of the mTHPC–PDT treatment was shown to be dependent on the drug release in the tumor tissue and on the drug localization.

The study shows that, in order to maximize the benefits of using liposomal carriers, a balance between drug delivery to the tumor and drug release from the liposomes must be achieved, as the absence of drug release will lead to the absence of the treatment effect, while the fast release of the drug from the carriers will not allow for sufficient drug accumulation in the tumor tissue. The development of a liposomal mTHPC formulation with modified release parameters compared to Fospeg®, including thermo- and ultrasound-sensitive liposomes, could be an attractive area for the continuation of the study.

Evidently, the parameters involved in the final efficacy of mTHPC-based PDT are extremely complex. The present study indicates that PEGylated liposomes appear to be more promising from a clinical point of view. A significant advantage of Fospeg®-PDT compared to Foslip® lies in a major decrease in DLI, while preserving the same PDT efficacy. Low accumulation of the drug in the skin, together with better efficacy at very short DLIs, could enhance the interest in PDT in outpatient settings.

## Acknowledgments

This work was supported by the Lorraine Cancer Institute research funds, PICS (International Program for Scientific Cooperation) grant 6032 (Belarusian grant No M12SP002), and Belarusian Republican Foundation for Fundamental Research grants (B11M-004, B11F-004, B13M-013). VR acknowledges the fellowship of the Ministry of Foreign and European Affairs of France. The authors thank Dr Alexander Stasheuski and Dr V Galievsky of the BI Stepanov Institute of Physics (Minsk, Belarus) for help with the singlet oxygen measurements.

## Disclosure

The authors report no conflicts of interest in this work.

## References

- Petros RA, DeSimone JM. Strategies in the design of nanoparticles for therapeutic applications. *Nat Rev Drug Discov*. 2010;9(8):615–627.
- Peer D, Karp JM, Hong S, Farokhzad OC, Margalit R, Langer R. Nanocarriers as an emerging platform for cancer therapy. *Nat Nanotechnol*. 2007;2(12):751–760.
- Torchilin VP. Recent advances with liposomes as pharmaceutical carriers. *Nat Rev Drug Discov*. 2005;4(2):145–160.
- Derycke AS, de Witte PA. Liposomes for photodynamic therapy. *Adv Drug Deliv Rev*. 2004;56(1):17–30.
- Chen B, Pogue BW, Hasan T. Liposomal delivery of photosensitising agents. *Expert Opin Drug Deliv*. 2005;2(3):477–487.
- Agostinis P, Berg K, Cengel KA, et al. Photodynamic therapy of cancer: an update. *CA Cancer J Clin*. 2011;61(4):250–281.
- Senge MO, Brandt JC. Temoporfin (Foscan®, 5,10,15,20-tetra(m-hydroxyphenyl)chlorin) – a second-generation photosensitizer. *Photochem Photobiol*. 2011;87(6):1240–1296.
- Compagnin C, Moret F, Celotti L, et al. Meta-tetra(hydroxyphenyl)chlorin-loaded liposomes sterically stabilised with poly(ethylene glycol) of different length and density: characterisation, in vitro cellular uptake and phototoxicity. *Photochem Photobiol Sci*. 2011;10(11):1751–1759.
- Buchholz J, Kaser-Hotz B, Khan T, et al. Optimizing photodynamic therapy: in vivo pharmacokinetics of liposomal meta-(tetrahydroxyphenyl)chlorin in feline squamous cell carcinoma. *Clin Cancer Res*. 2005;11(20):7538–7544.
- Buchholz J, Wergin M, Walt H, Gräfe S, Bley CR, Kaser-Hotz B. Photodynamic therapy of feline cutaneous squamous cell carcinoma using a newly developed liposomal photosensitizer: preliminary results concerning drug safety and efficacy. *J Vet Intern Med*. 2007;21(4):770–775.
- Bovis MJ, Woodhams JH, Loizidou M, Scheglmann D, Bown SG, MacRobert AJ. Improved in vivo delivery of m-THPC via pegylated liposomes for use in photodynamic therapy. *J Control Release*. 2012;157(2):196–205.
- de Visscher SA, Kaščáková S, de Bruijn HS, et al. Fluorescence localization and kinetics of mTHPC and liposomal formulations of mTHPC in the window-chamber tumor model. *Lasers Surg Med*. 2011;43(6):528–536.
- Pegaz B, Debeve E, Ballini JP, et al. Photothrombic activity of m-THPC-loaded liposomal formulations: pre-clinical assessment on chick chorioallantoic membrane model. *Eur J Pharm Sci*. 2006;28(1–2):134–140.
- Decker C, Schubert H, May S, Fahr A. Pharmacokinetics of temoporfin-loaded liposome formulations: correlation of liposome and temoporfin blood concentration. *J Control Release*. 2013;166(3):277–285.

15. Allen TM, Cheng WW, Hare JJ, Laginha KM. Pharmacokinetics and pharmacodynamics of lipidic nano-particles in cancer. *Anticancer Agents Med Chem*. 2006;6(6):513–523.
16. Mitra S, Maugain E, Bolotine L, Guillemin F, Foster TH. Temporally and spatially heterogeneous distribution of mTHPC in a murine tumor observed by two-color confocal fluorescence imaging and spectroscopy in a whole-mount model. *Photochem Photobiol*. 2005;81(5):1123–1130.
17. Reshetov V, Kachatkou D, Shmigol T, et al. Redistribution of meta-tetra(hydroxyphenyl)chlorin (m-THPC) from conventional and PEGylated liposomes to biological substrates. *Photochem Photobiol Sci*. 2011;10(6):911–919.
18. Coutier S, Bezdetnaya LN, Foster TH, Parache RM, Guillemin F. Effect of irradiation fluence rate on the efficacy of photodynamic therapy and tumor oxygenation in meta-tetra (hydroxyphenyl) chlorin (mTHPC)-sensitized HT29 xenografts in nude mice. *Radiat Res*. 2002;158(3):339–345.
19. Lassalle HP, Dumas D, Gräfe S, D'Hallewin MA, Guillemin F, Bezdetnaya L. Correlation between in vivo pharmacokinetics, intratumoral distribution and photodynamic efficiency of liposomal mTHPC. *J Control Release*. 2009;134(2):118–124.
20. Clark B, Smith DA, editors. *An Introduction to Pharmacokinetics*. 2nd ed. Oxford, UK: Blackwell Scientific; 1986.
21. Kachatkou D, Sasnouski S, Zorin V, et al. Unusual photoinduced response of mTHPC liposomal formulation (Foslip). *Photochem Photobiol*. 2009;85(3):719–724.
22. Filipe V, Hawe A, Jiskoot W. Critical evaluation of Nanoparticle Tracking Analysis (NTA) by NanoSight for the measurement of nanoparticles and protein aggregates. *Pharm Res*. 2010;27(5):796–810.
23. Reshetov V, Zorin V, Siupa A, D'Hallewin MA, Guillemin F, Bezdetnaya L. Interaction of liposomal formulations of meta-tetra(hydroxyphenyl)chlorin (temoporfin) with serum proteins: protein binding and liposome destruction. *Photochem Photobiol*. 2012;88(5):1256–1264.
24. Dumas D, Hupont S, Huselstein C, et al. SHG as a new modality for large field of view imaging to monitor tissue collagen network. *Biomed Mater Eng*. 2012;22(1–3):159–162.
25. Malgady RG, Krebs DB. Understanding correlation coefficients and regression. *Phys Ther*. 1986;66(1):110, 112, 114 passim.
26. Taylor R. Interpretation of the correlation coefficient: a basic review. *J Diagn Med Sonogr*. 1990;6(1):35–39.
27. Drummond DC, Noble CO, Hayes ME, Park JW, Kirpotin DB. Pharmacokinetics and in vivo drug release rates in liposomal nanocarrier development. *J Pharm Sci*. 2008;97(11):4696–4740.
28. Kuntsche J, Freisleben I, Steiniger F, Fahr A. Temoporfin-loaded liposomes: physicochemical characterization. *Eur J Pharm Sci*. 2010;40(4):305–315.
29. Hefesha H, Loew S, Liu X, May S, Fahr A. Transfer mechanism of temoporfin between liposomal membranes. *J Control Release*. 2011;150(3):279–286.
30. Ogihara-Umeda I, Kojima S. Increased delivery of gallium-67 to tumors using serum-stable liposomes. *J Nucl Med*. 1988;29(4):516–523.
31. Harashima H, Hiraiwa T, Ochi Y, Kiwada H. Size dependent liposome degradation in blood: in vivo/in vitro correlation by kinetic modeling. *J Drug Target*. 1995;3(4):253–261.
32. Ishida T, Funato K, Kojima S, Yoda R, Kiwada H. Enhancing effect of cholesterol on the elimination of liposomes from circulation is mediated by complement activation. *Int J Pharm*. 1997;156(1):27–37.
33. Taurin S, Nehoff H, Greish K. Anticancer nanomedicine and tumor vascular permeability; Where is the missing link? *J Control Release*. 2012;164(3):265–275.
34. Papahadjopoulos D, Allen TM, Gabizon A, et al. Sterically stabilized liposomes: improvements in pharmacokinetics and antitumor therapeutic efficacy. *Proc Natl Acad Sci U S A*. 1991;88(24):11460–11464.
35. Bourdon O, Laville I, Carrez D, et al. Biodistribution of meta-tetra(hydroxyphenyl)chlorin incorporated into surface-modified nanocapsules in tumor-bearing mice. *Photochem Photobiol Sci*. 2002;1(9):709–714.
36. Star WM, Marijnissen HP, van den Berg-Blok AE, Versteeg JA, Franken KA, Reinhold HS. Destruction of rat mammary tumor and normal tissue microcirculation by hematoporphyrin derivative photoradiation observed in vivo in sandwich observation chambers. *Cancer Res*. 1986;46(5):2532–2540.
37. Heldin CH, Rubin K, Pietras K, Ostman A. High interstitial fluid pressure – an obstacle in cancer therapy. *Nat Rev Cancer*. 2004;4(10):806–813.
38. Garrier J, Bressenot A, Gräfe S, et al. Compartmental targeting for mTHPC-based photodynamic treatment in vivo: Correlation of efficiency, pharmacokinetics, and regional distribution of apoptosis. *Int J Radiat Oncol Biol Phys*. 2010;78(2):563–571.

## Supplementary materials

**Table S1** Measurements of singlet oxygen generation yield of liposomal mTHPC

Luminescence of singlet oxygen at 1,270 nm was measured on a custom laser near infrared lifetime spectrometer developed at the Institute of Physics of the National Academy of Sciences of Belarus. The detection system of the setup is based on the advanced photon counting method. Luminescence radiation was collected with a high-throughput optical system and directed to H10330-45 PMT (Hamamatsu Photonics K.K., Iwata, Japan) via MS2004i monochromator (SOLAR TII Ltd, Minsk, Belarus). The signal was processed by P7888-2 multiscaler (FAST ComTec GmbH, Oberhaching, Germany), with the channel width set to 64 ns. Samples were excited by laser pulses at a wavelength of 531 nm (STA-01SH Nd:LSB laser; STANDA, Ltd, Vilnius, Lithuania), with a pulse energy of 3  $\mu$ J, a pulse duration of 0.7 ns, and a repetition rate of 1 kHz.

The quantum yield of the singlet oxygen photosensitized generation of meta-tetra(hydroxyphenyl)chlorin (mTHPC) in liposomes was determined using the reference-comparison method by detecting luminescence kinetic signals after pulsed laser excitation. As a standard, 5,10,15,20-Tetrakis(N-methyl-4-pyridyl)-21H,23H-porphine was used, with a quantum yield of singlet oxygen generation in the aqueous solution of 0.77. The total amount of excitation pulses was  $3 \times 10^5$ . To minimize sample photodegradation, continuous magnetic stirring was used. Sample photostability was verified with a photodiode during experiments by the intensity of laser radiation transmitted through a sample and with a spectrophotometer before and after the experiment. Within the signal accumulation time (300 seconds) the optical density of the samples decreased by less than 5%. Signal intensities were extrapolated from the fitting of data with the difference of two exponential decay functions. After that, signal intensities were corrected for absorption of the samples at the laser wavelength, and the singlet oxygen quantum yield was calculated according to:

$$QY^{\text{sample}} = QY^{\text{st}} \frac{I^{\text{sample}}}{I^{\text{st}}} \frac{(1 - 10^{-OD})_{532}^{\text{st}}}{(1 - 10^{-OD})_{532}^{\text{sample}}}, \quad (1)$$

where  $QY^{\text{sample}}$  ( $QY^{\text{st}}$ ) is the singlet oxygen quantum yield of the sample (standard),  $I^{\text{sample}}$  ( $I^{\text{st}}$ ) is the sample (standard) extrapolated signal intensity, and  $OD^{\text{sample}}$  ( $OD^{\text{st}}$ ) is the optical density of the sample (standard) at 531 nm.

A series of dipalmitoylphosphatidylcholine/dipalmitoylphosphatidylglycerol liposomes was prepared according to the method described in the article, with the lipid:mTHPC ratios (mol/mol) from 10:1 to 400:1. Two independent series of experiments were conducted, and the averaged results of singlet oxygen generation quantum yield are displayed in Figure S4.

### Photoinduced fluorescence quenching

Irradiation of mTHPC liposomal formulations at low light doses induces a significant fluorescence decrease, followed by its restoration after the addition of a detergent. We attributed this behavior to photoinduced fluorescence quenching. The value of normalized fluorescence was used as an indicator of photoinduced quenching. Normalized fluorescence was defined as the ( $I/I_{X-100}$ ) ratio, where ( $I$ ) is the mTHPC fluorescence intensity measured immediately after irradiation and ( $I_{X-100}$ ) is the mTHPC fluorescence intensity measured after addition of 0.2% Triton<sup>®</sup> X-100 (Sigma-Aldrich, St Louis, MO, USA) to the same sample. All photoinduced fluorescence quenching measurements were done in triplicate.

As previously described,<sup>17</sup> the experimental normalized fluorescence value obtained during Foslip<sup>®</sup> (Biolitec Research GmbH, Jena, Germany) or Fospeg<sup>®</sup> (Biolitec Research GmbH) incubation in plasma ( $\Delta_{\text{exp}}[t]$ ) corresponds to the sum of normalized fluorescence values in donor liposomes ( $\Delta_{\text{donor}}[C(t)/C_0]$ ) and acceptor structures ( $\Delta_{\text{acceptor}}$ ) with appropriate weighting factors:

$$\Delta_{\text{exp}}(t) = C(t)/C_0 \cdot \Delta_{\text{donor}}(C(t)/C_0) + (C_0 - C(t))/C_0 \cdot \Delta_{\text{acceptor}} \quad (2)$$

where  $C_0$  is the initial mTHPC concentration in Foslip<sup>®</sup> or Fospeg<sup>®</sup>, and  $C(t)$  stands for the mTHPC concentration in Foslip<sup>®</sup> or Fospeg<sup>®</sup> liposomes during incubation. In addition,  $\Delta_{\text{donor}}(C(t)/C_0)$  is derived from independent measurements of normalized fluorescence of liposomes with different dye:lipid ratios in buffer – ie, a calibration curve of the amplitude of photoinduced fluorescence quenching in the liposomes prepared by extrusion with different drug:lipid ratios. Therefore, the  $C(t)/C_0$  ratio may be calculated as follows:

$$C(t)/C_0 = (\Delta_{\text{acceptor}} - \Delta_{\text{exp}}[t]) / (\Delta_{\text{acceptor}} - \Delta_{\text{donor}}[C(t)/C_0]) \quad (3)$$

Equation 3 was solved using a numerical method, taking into account that  $\Delta_{\text{acceptor}}$  is equal to 1 (as no photoinduced fluorescence quenching was attributed to mTHPC in acceptor structures due to their excessive amount). This approach allowed us to calculate the amount of mTHPC residing in liposomes at each time point, as well as the percentage of mTHPC released from the carriers.

The measurement of photoinduced fluorescence-quenching amplitude in the plasma samples of Foslip<sup>®</sup> and Fospeg<sup>®</sup> injected in mice are shown in Figure S5.

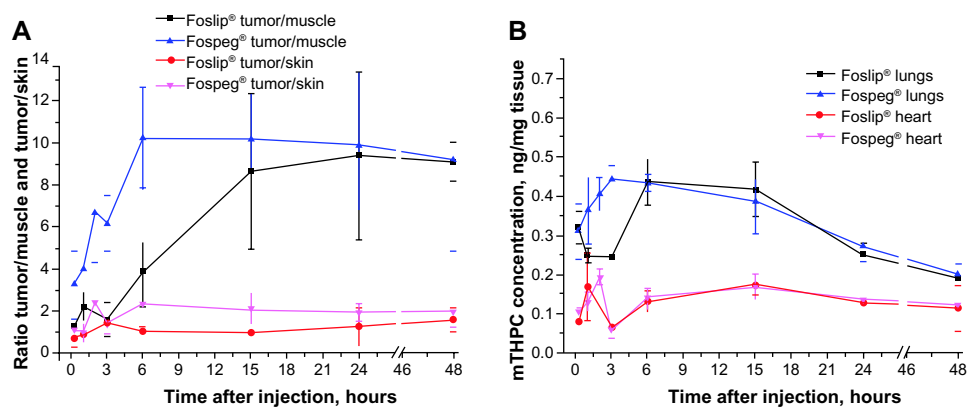


**Figure S1** Tumor/muscle and tumor/skin ratios, as well as the concentration of mTHPC in the lungs and heart.

**Notes:** (A) Tumor/muscle and tumor/skin ratios; (B) concentration of mTHPC in the lungs and heart as a function of time following injection of Foslip® or Fospeg®.

\*Biolitec Research GmbH, Jena, Germany.

**Abbreviation:** mTHPC, meta-tetra(hydroxyphenyl)chlorin.

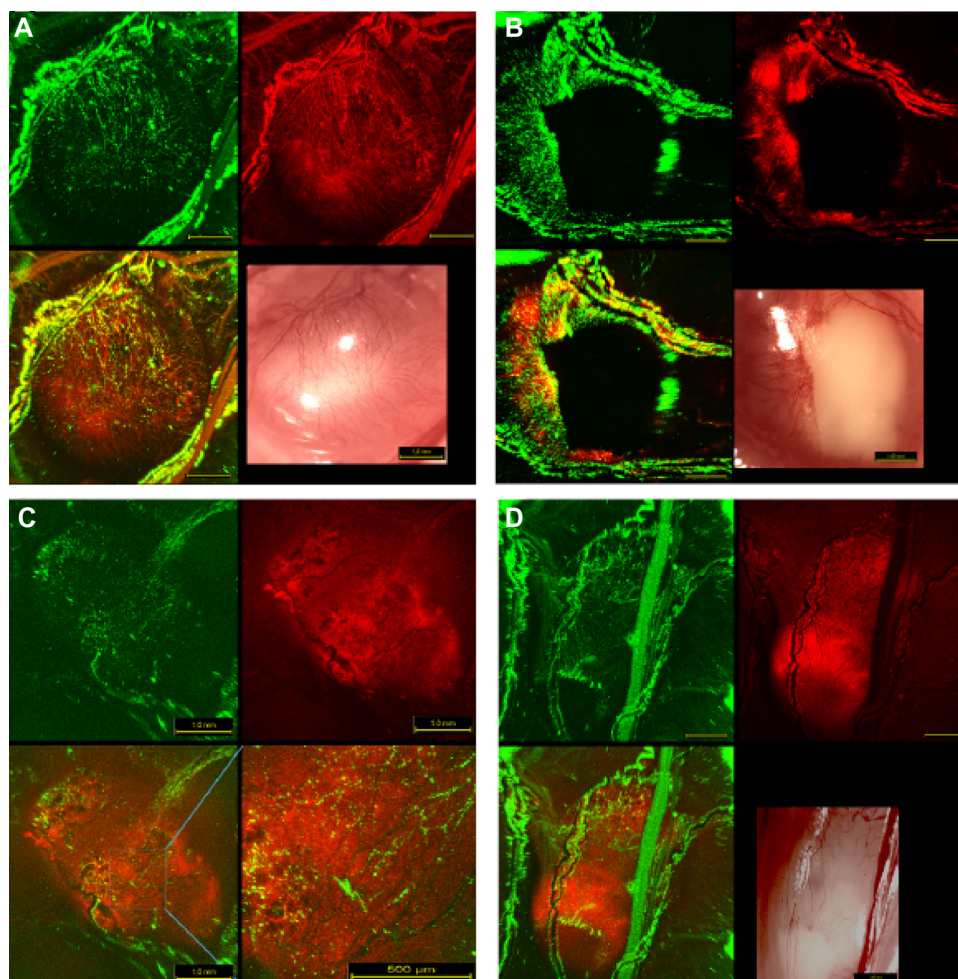


**Figure S2** Representative in vivo multiphoton confocal and white-light microscopy images of whole HT29 tumors.

**Notes:** Images were acquired (A) 3 hours, (B) 6 hours, (C) 15 hours, and (D) 24 hours following the injection of 7.5 mg/kg mTHPC in the form of Foslip® (Biolitec Research GmbH, Jena, Germany). Vascular perfusion marker fluorescence is shown in the green false color, mTHPC fluorescence is shown in red. The lower left image of each block is the overlay of the green and red channels. (C) The zoomed region of the overlay image is shown instead of a white-light image. The scale bar value shown on the white-light image applies to all four images.

**Abbreviation:** mTHPC, meta-tetra(hydroxyphenyl)chlorin.

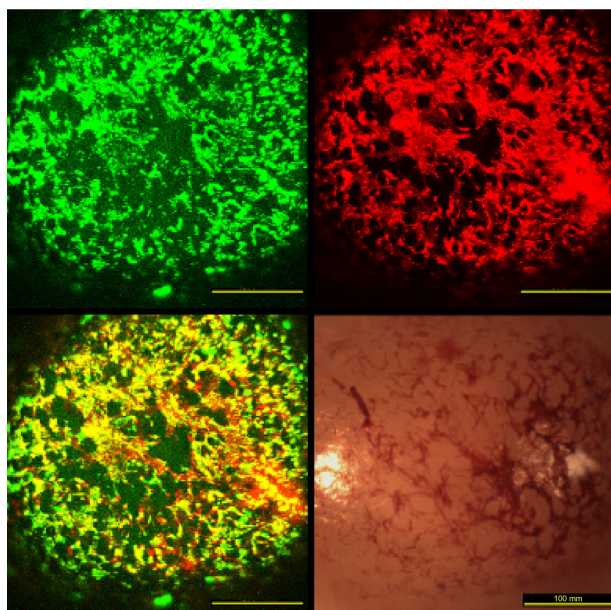


**Figure S3** In vivo multiphoton confocal and white-light macroscopy images of whole HT29 tumor acquired 30 minutes following the injection of 7.5 mg/kg of mTHPC in the form of Fospeg®/Foslip® (Biolitec Research GmbH, Jena, Germany).

**Notes:** Vascular perfusion marker fluorescence is shown in the green false color, and mTHPC fluorescence is shown in red. The lower left image is the overlay of the green and red channels. The scale bar value shown on the white-light image applies to the whole block.

**Abbreviation:** mTHPC, meta-tetra(hydroxyphenyl)chlorin.

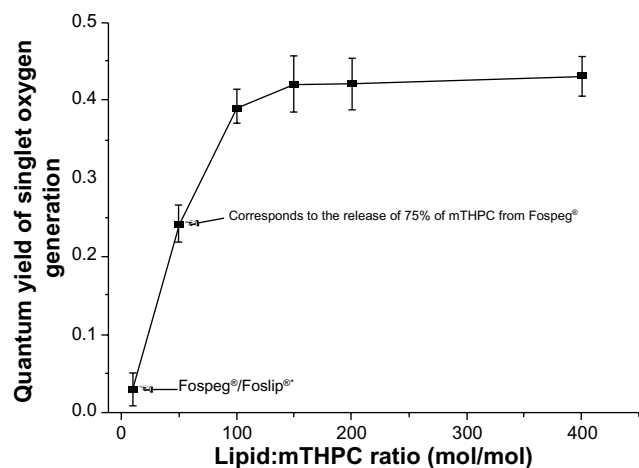


**Figure S4** Singlet oxygen generation yield by liposomal mTHPC at different lipid:drug ratios.

**Note:** \*Biolitec Research GmbH, Jena, Germany.

**Abbreviation:** mTHPC, meta-tetra(hydroxyphenyl)chlorin.

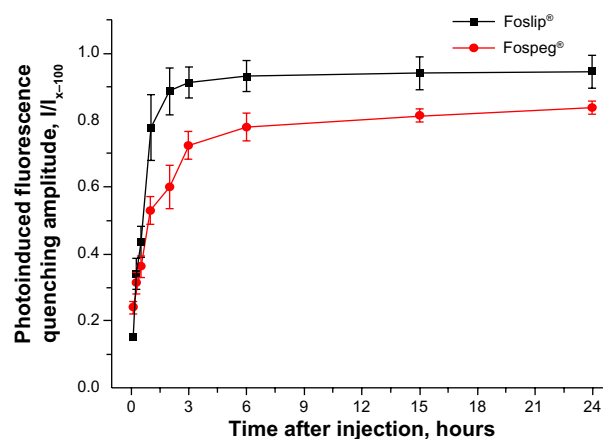


**Figure S5** Photoinduced quenching of mTHPC in Foslip®\* and Fospeg®\* in the blood circulation after injection into tumor-bearing mice.

**Note:** \*Biolitec Research GmbH, Jena, Germany.

**Abbreviation:** mTHPC, meta-tetra(hydroxyphenyl)chlorin.

International Journal of Nanomedicine

Publish your work in this journal

The International Journal of Nanomedicine is an international, peer-reviewed journal focusing on the application of nanotechnology in diagnostics, therapeutics, and drug delivery systems throughout the biomedical field. This journal is indexed on PubMed Central, MedLine, CAS, SciSearch®, Current Contents®/Clinical Medicine,

Submit your manuscript here: <http://www.dovepress.com/international-journal-of-nanomedicine-journal>

Dovepress

Journal Citation Reports/Science Edition, EMBase, Scopus and the Elsevier Bibliographic databases. The manuscript management system is completely online and includes a very quick and fair peer-review system, which is all easy to use. Visit <http://www.dovepress.com/testimonials.php> to read real quotes from published authors.